

HERMETIC PACKAGES AND FEEDTHROUGHS FOR NEURAL PROSTHESES

Quarterly Progress Report # 13

(Contract NIH-NINDS-N01-NS-4-2319)

(Contractor: The Regents of the University of Michigan)

For the Period:

October- December 1997

Submitted to the

*Neural Prosthesis Program
National Institute of Neurological Disorders and Stroke
National Institutes of Health*

By the

*Center For Integrated Sensors and Circuits
Department of Electrical Engineering and Computer Science
University of Michigan
Ann Arbor, Michigan 48109-2122*

Program Personnel:

UNIVERSITY OF MICHIGAN

Professor Khalil Najafi: Principal Investigator

Graduate Student Research Assistants:

Mr. Mehmet Dokmeci: Packaging and Accelerated Testing

Mr. Jeffrey Von Arx: Electrode and Package Fabrication/Testing

Mr. Sebastien Hauvespre: Package Fabrication and Testing

VANDERBILT UNIVERSITY

Professor David L. Zeale, Principal Investigator

January 1998

SUMMARY

During the past quarter we continued testing of glass packages under accelerated conditions, continued and completed the fabrication of the receiver circuitry for the single-channel microstimulator and fully integrated multichannel nerve stimulation system. Preliminary tests on these wafers have shown that both microstimulators and nerve stimulation systems are fully functional.

Our most significant package testing results to date are those obtained from a series of silicon-glass packages that have been soaking in DI water at 85°C and 95°C for more than a year. We reported in the last progress reports that all packages soaking at 95°C had failed. There were also 4 packages that were soaking at 85°C. All these four packages are still dry and under test. Of the original 10 packages, the longest going sample has reached a maximum of 1190 days at 85°C and 484 days at 95°C. If we assume that all of the packages at 85°C failed the same time that the 95°C packages failed, we can calculate a worst case MTTF at body temperature of 59 years. These tests have been very encouraging and clearly indicate the packages can last for many years in water. In addition to these tests in DI water, we had also soaked several packages in *saline* at the above two temperatures. The results obtained from these tests were reported in the last progress report. We also have had 4 packages soaking at room temperature in saline. The longest lasting package has been soaking for 1090 days, and an average soak period of 897 days at room temperature. We will continue to observe these packages for any sign of leakage. A new set of package tests were also initiated this past quarter at 85 and 95°C. At each temperature, eight packages that have been coated with silicone to prevent premature dissolution of the top polysilicon bonding layer have now been soaking for 126 days each. Only one package at 85°C failed after the first day due to premature failure and possible damage in the bond area. Three of the packages soaking at 95°C failed this past quarter due to the dissolution of the polysilicon layer. The other packages are still under test.

In-vivo testing of these packages continued at Michigan, Johns Hopkins University, and Vanderbilt University by Dr. Zeale's group. All of these tests indicate that the silicon-glass package is indeed biocompatible and does not induce any damage in the surrounding tissue. A detailed description of these results will be presented in the final report once all the data is available.

Finally, during the past quarter we completed the fabrication of the muscular microstimulator, and the fully integrated 8-channel mini-microstimulator that can operate using on-chip coils. This circuitry can be used for peripheral nerve stimulation applications and can deliver current pulses to any of 8 electrodes. The first wafers have just come out of fabrication and tests have been performed on both circuits. Both circuits function as expected. The single-channel microstimulator function with a current draw of about 1.7-1.9mA, as designed, and delivers stimulus pulses as required. This circuit will be assembled on complete microstimulators for further telemetry testing. The nerve stimulation system has also been tested and it is also shown to be fully functional. The circuit delivers a fully programmable pulse duration and amplitude current pulse through eight channels. The chip will function using an on-chip coil which will be integrated on the chip during the coming quarter. We consider both of these results extremely significant and hope that we can develop and provide a number of actual units to our collaborators for further testing. The results of these tests will be presented in the final report for this contract.

1. INTRODUCTION

This project deals with the development of hermetic, biocompatible micropackages and feedthroughs for use in a variety of implantable neural prostheses for sensory and motor handicapped individuals. The project also aims at continuing work on the development of a telemetrically powered and controlled neuromuscular microstimulator for functional electrical stimulation. The primary objectives of the project are: 1) the development and characterization of hermetic packages for miniature, silicon-based, implantable three-dimensional structures designed to interface with the nervous system for periods of up to 40 years; 2) the development of techniques for providing multiple sealed feedthroughs for the hermetic package; 3) the development of custom-designed packages and systems used in chronic stimulation or recording in the central or peripheral nervous systems in collaboration and cooperation with groups actively involved in developing such systems; and 4) establishing the functionality and biocompatibility of these custom-designed packages in *in-vivo* applications. Although the project is focused on the development of the packages and feedthroughs, it also aims at the development of inductively powered systems that can be used in many implantable recording/stimulation devices in general, and of multichannel microstimulators for functional neuromuscular stimulation in particular.

Our group here at the Center for Integrated Sensors and Circuits at the University of Michigan has been involved in the development of silicon-based multichannel recording and stimulating microprobes for use in the central and peripheral nervous systems. More specifically, during the past two contract periods dealing with the development of a single-channel inductively powered microstimulator, our research and development program has made considerable progress in a number of areas related to the above goals. A hermetic packaging technique based on electrostatic bonding of a custom-made glass capsule and a supporting silicon substrate has been developed and has been shown to be hermetic for a period of at least a few years in salt water environments. This technique allows the transfer of multiple interconnect leads between electronic circuitry and hybrid components located in the sealed interior of the capsule and electrodes located outside of the capsule. The glass capsule can be fabricated using a variety of materials and can be made to have arbitrary dimensions as small as 1.8mm in diameter. A multiple sealed feedthrough technology has been developed that allows the transfer of electrical signals through polysilicon conductor lines located on a silicon support substrate. Many feedthroughs can be fabricated in a small area. The packaging and feedthrough techniques utilize biocompatible materials and can be integrated with a variety of micromachined silicon structures.

The general requirements of the hermetic packages and feedthroughs to be developed under this project are summarized in Table 1. Under this project we will concentrate our efforts to satisfy these requirements and to achieve the goals outlined above. There are a variety of neural prostheses used in different applications, each having different requirements for the package, the feedthroughs, and the particular system application. The overall goal of the program is to develop a miniature hermetic package that can seal a variety of electronic components such as capacitors and coils, and integrated circuits and sensors (in particular electrodes) used in neural prostheses. Although the applications are different, it is possible to identify a number of common requirements in all of these applications in addition to those requirements listed in Table 1. The packaging and feedthrough technology should be capable of:

- 1- protecting non-planar electronic components such as capacitors and coils, which typically have large dimensions of about a few millimeters, without damaging them;
- 2- protecting circuit chips that are either integrated monolithically or attached in a hybrid fashion with the substrate that supports the sensors used in the implant;
- 3- interfacing with structures that contain either thin-film silicon microelectrodes or conventional microelectrodes that are attached to the structure;

Table 1: General Requirements for Miniature Hermetic Packages and Feedthroughs for Neural Prostheses Applications

Package Lifetime:

≥ 40 Years in Biological Environments @ 37°C

Packaging Temperature:

≤360°C

Package Volume:

10-100 cubic millimeters

Package Material:

Biocompatible

Transparent to Light

Transparent to RF Signals

Package Technology:

Batch Manufactureable

Package Testability:

Capable of Remote Monitoring

In-Situ Sensors (Humidity & Others)

Feedthroughs:

At Least 12 with ≤125μm Pitch

Compatible with Integrated or Hybrid Microelectrodes

Sealed Against Leakage

Testing Protocols:

In-Vitro Under Accelerated Conditions

In-Vivo in Chronic Recording/Stimulation Applications

We have identified two general categories of packages that need to be developed for implantable neural prostheses. The first deals with those systems that contain large components like capacitors, coils, and perhaps hybrid integrated circuit chips. The second deals with those systems that contain only integrated circuit chips that are either integrated in the substrate or are attached in a hybrid fashion to the system.

Figure 1 shows our general proposed approach for the package required in the first category. This figure shows top and cross-sectional views of our proposed approach here. The package is a glass capsule that is electrostatically sealed to a support silicon substrate. Inside the glass capsule are housed all of the necessary components for the system. The electronic circuitry needed for any analog or digital circuit functions is either fabricated on a separate circuit chip that is hybrid mounted on the silicon substrate and electrically connected to the silicon substrate, or integrated monolithically in the support silicon substrate itself. The attachment of the hybrid IC chip to the silicon substrate can be performed using a number of different technologies such as simple wire bonding between pads located on each substrate, or using more sophisticated techniques such as flip-chip solder reflow or tab bonding. The larger capacitor or microcoil components are mounted on either the substrate or the IC chip using appropriate epoxies or solders. This completes the assembly of the electronic components of the system and it should be possible to test the system electronically at this point before the package is completed. After testing, the system is packaged by placing the glass capsule over the entire system and bonding it to the silicon substrate using an electrostatic sealing process. The cavity inside the glass package is now hermetically sealed against the outside environment. Feedthroughs to the outside world are provided using the grid-feedthrough technique discussed in previous reports. These feedthroughs transfer the electrical signals between the electronics inside the package and various elements outside of the package. If the package has to interface with conventional microelectrodes, these microelectrodes can be attached to bonding pads located outside of the package; the bond junctions will have to be protected from the external environment using various polymeric encapsulants. If the package has to interface with on-chip electrodes, it can do so by integrating the electrode on the silicon support substrate. Interconnection is simply achieved using on-chip polysilicon conductors that make the feedthroughs themselves. If the package has to interface with remotely located recording or stimulating electrodes that are attached to the package using a silicon ribbon cable, it can do so by integrating the cable and the electrodes again with the silicon support substrate that houses the package and the electronic components within it.

Figure 2 shows our proposed approach to package development for the second category of applications. In these applications, there are no large components such as capacitors and coils. The only component that needs to be hermetically protected is the electronic circuitry. This circuitry is either monolithically fabricated in the silicon substrate that supports the electrodes (similar to the active multichannel probes being developed by the Michigan group), or is hybrid attached to the silicon substrate that supports the electrodes (like the passive probes being developed by the Michigan group). In both of these cases the package is again another glass capsule that is electrostatically sealed to the silicon substrate. Notice that in this case, the glass package need not be a high profile capsule, but rather it need only have a cavity that is deep enough to allow for the silicon chip to reside within it. Note that although the silicon IC chip is originally 500 μm thick, it can be thinned down to about 100 μm , or can be recessed in a cavity created in the silicon substrate itself. In either case, the recess in the glass is less than 100 μm deep (as opposed to several millimeters for the glass capsule). Such a glass package can be easily fabricated in a batch process from a larger glass wafer.

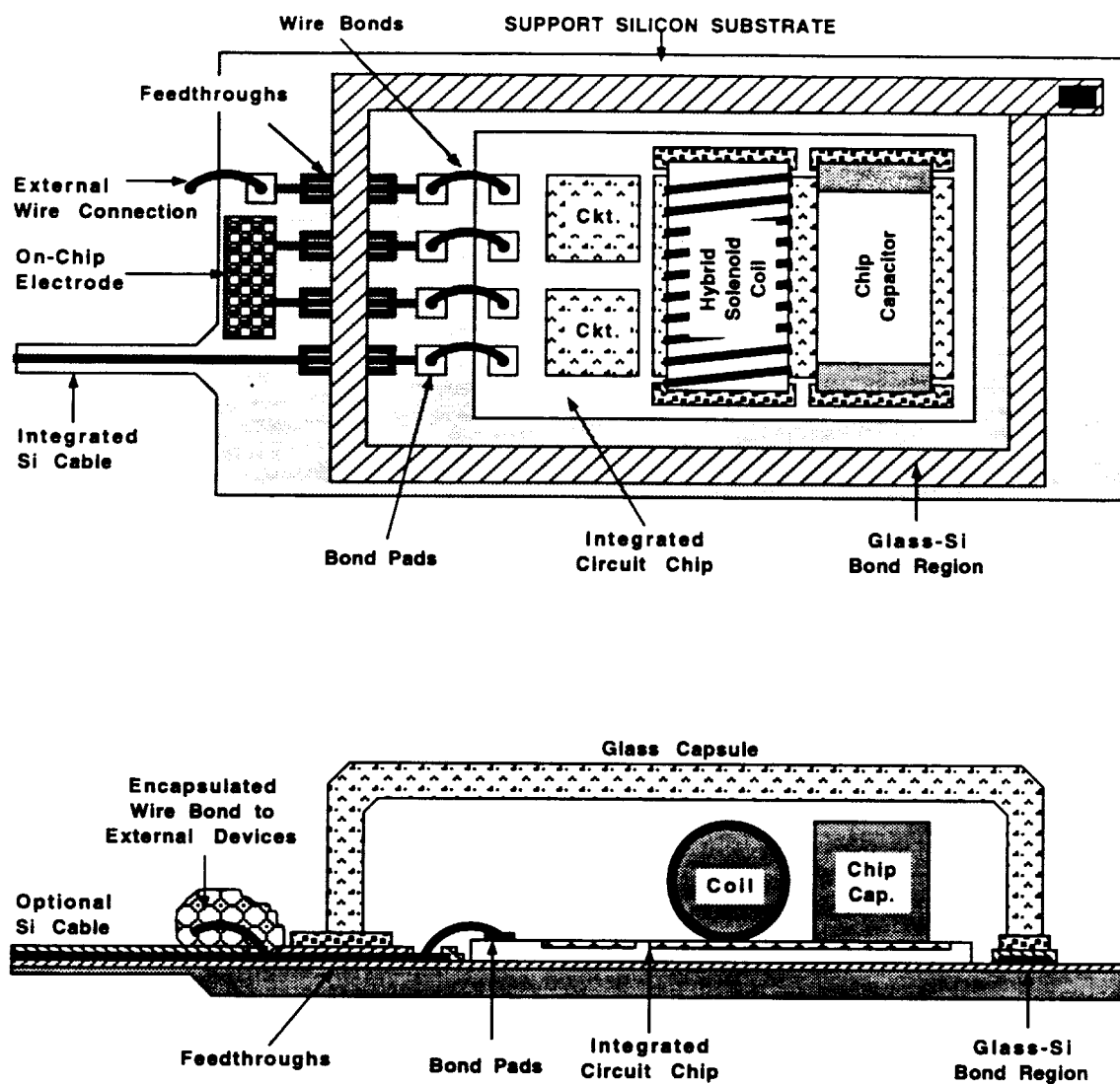


Figure 1: A generic approach for packaging implantable neural prostheses that contain a variety of components such as chip capacitors, microcoils, and integrated circuit chips. This packaging approach allows for connecting to a variety of electrodes.

We believe the above two approaches address the needs for most implantable neural prostheses. Note that both of these techniques utilize a silicon substrate as the supporting base, and are not directly applicable to structures that use other materials such as ceramics or metals. Although this may seem a limitation at first, we believe that the use of silicon is, in fact, an advantage because it provides several benefits. First, it is biocompatible and has been used extensively in biological applications. Second, there is a great deal of effort in the IC industry in the development of multi-chip modules (MCMs), and many of these efforts use silicon supports because of the ability to form high density interconnections on silicon using standard IC fabrication techniques. Third, many present and future implantable probes are based on silicon micromachining technology; the use of our proposed packaging technology is inherently compatible with most of these probes, which simplifies the overall structure and reduces its size.

Once the above packages are developed, we will test them in biological environments by designing packages for specific applications. One of these applications is in recording neural activity from cortex using silicon microprobes developed by the Michigan group under separate contracts. The other involves the chronic stimulation of muscular tissue using a multichannel microstimulator for the stimulation of the paralyzed larynx. This application has been developed at Vanderbilt University. Once the device is built, it will be used by our colleagues at Vanderbilt to perform both biocompatibility tests and functional tests to determine package integrity and suitability and device functionality for the reanimation of the paralyzed larynx. The details of this application will be discussed in future progress reports.

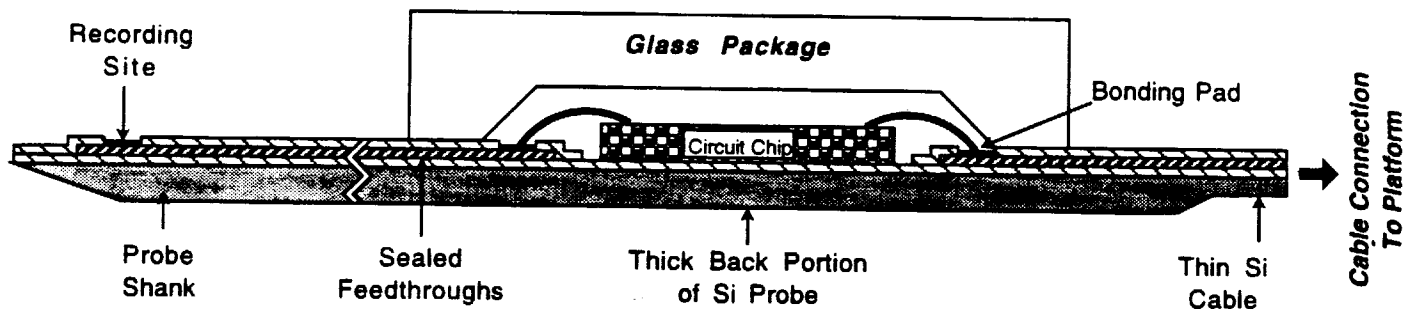


Figure 2: Proposed packaging approach for implantable neural prostheses that contain electronic circuitry, either monolithically fabricated in the probe substrate or hybrid attached to the silicon substrate containing microelectrodes.

2. ACTIVITIES DURING THE PAST QUARTER

2.1 Hermetic Packaging

Over the past few years we have developed a bio-compatible hermetic package with high density multiple feedthroughs. This technology utilizes electrostatic bonding of a custom-made glass capsule to a silicon substrate to form a hermetically sealed cavity, as shown in Figure 3. Feedthrough lines are obtained by forming closely spaced polysilicon lines and planarizing them with LTO and PSG. The PSG is reflowed in steam at 1100°C for 2 hours to form a planarized surface. A passivation layer of oxide/nitride/oxide is then deposited on top to prevent direct exposure of PSG to moisture. A layer of fine-grain polysilicon (surface roughness 50Å rms) is deposited and doped to act as the bonding surface. Finally, a glass capsule is bonded to this top polysilicon layer by applying a voltage of 2000V between the two for 10 minutes at 320 to 340°C, a temperature compatible with most hybrid components. The glass capsule can be either custom molded from Corning code #7740 glass, or can be batch fabricated using ultrasonic micromachining of #7740 glass wafers.

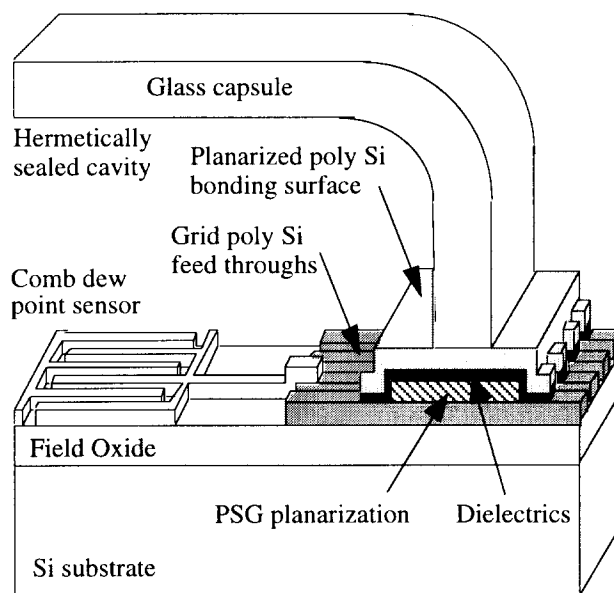


Figure 3: The structure of the hermetic package with grid feedthroughs.

During the past years we have electrostatically bonded and soak tested over one hundred and sixty of these packages. The packages successfully prevent leakage in soak tests at 95°C for over 4 months on average and at 85° C for 20 months in deionized water. The bonding yield is about 82% (yield is defined as the percentage of packages which last more than 24 hours in the solution they are soaked in). We also would like to mention that the earlier tests that have been going for more than about 3 years (room temperature soak tests in saline and the 85° C and the 95°C tests in deionized water) have been made with silicon substrates that were thinned (~150µm) and bonded to the custom molded glass capsules. All of the relatively recent tests (85° C and 95°C tests in saline) are performed with the silicon substrates having full thickness (~500µm) and bonded to the ultrasonically machined glass capsules with a flat top surface. We currently have devices tested in deionized water for over 3 years at 85° C. A set of devices have been coated with a silicone polymer and were soaked in saline during the previous quarter. These samples are currently under test which will be detailed in a later section of this report. In-vivo test results from the package reveal that the devices are biocompatible and rugged. Using a wafer with a thin layer of evaporated glass and a silicon substrate, we also fabricated an all

silicon package and pull tests performed on the package indicate that the strength of this bond is similar to the bonds made to bulk glass. We have also sent several devices to our collaborators for biocompatibility tests which we will report as they become available.

2.1.1 Ongoing Accelerated Soak Tests in Deionized Water

We have continued our accelerated soak tests during this quarter. At the present time, out of the original 20 packages we have 4 packages that have lasted for more than three and a quarter years of testing time with no sign of moisture penetration inside them. In these tests temperature is chosen as the accelerating factor since it is easy to control and also the diffusion of moisture is a strong(exponential) function of temperature. We had started soaking 10 samples each at 85°C and 95°C. Tables 2 and 3 below list some pertinent data from these soak tests. Figure 4 summarizes the final results from the 95°C soak tests and Figure 5 summarizes the results so far from the 85°C tests. These figures also list the causes of failure for individual packages when it is known, and they show a curve fit to our lifetime data to illustrate the general trend. The curve fit, however, only approximates the actual package lifetimes since some of our packages failed due to breaking during testing rather than due to leakage.

At the beginning of this quarter, we had 4 packages soaking at 85°C. These packages are still dry and under test. For these packages we define failure as the room temperature condensation of moisture inside the package. The testing sequence for these packages start by cooling the sample to room temperature from its soak bath at the elevated temperature. The samples are next rinsed with deionized water and then dried with a nitrogen gun. We then measure the impedance of the dew point sensors and inspect the sample carefully for leakage under the microscope. The significant change in impedance (about 2 orders of magnitude) and observation of visible condensation inside the package would both be classified as the failure of the package under test. Of the original 10 samples in the 95°C tests, the longest lasting package survived for a total of 484 days. The calculated mean time to failure of these packages are 135.7 days excluding the handling errors. Of the original 10 packages in the 85°C soak tests there are still 4 with no sign of room temperature condensation. The longest lasting package in the 85°C tests has lasted a total of 1190 days and is still under test. The worst case mean time to failure for these tests has been calculated as 942 days excluding the handling errors. We have also started new soak tests in saline which would be detailed in a following section.

Table 2: Key data for 95°C soak tests in DI water.

Number of packages in this study	10
Soaking solution	DI water
Failed within 24 hours (not included in MTTF)	1
Packages lost due to mishandling	2
Longest lasting packages in this study	484 days
Packages still under tests with no measurable room temperature condensation inside	0
Average lifetime to date (MTTF) including losses attributed to mishandling	118.7 days
Average lifetime to date (MTTF) not including losses attributed to mishandling	135.7 days

Table 3: Key data for 85°C soak tests in DI water.

Number of packages in this study	10
Soaking solution	DI water
Failed within 24 hours (not included in MTF)	2
Packages lost due to mishandling	3
Longest lasting packages so far in this study	1190 days
Packages still under tests with no measurable room temperature condensation inside	4
Average lifetime to date (MTTF) including losses attributed to mishandling	599 days
Average lifetime to date (MTTF) not including losses attributed to mishandling	941.8 days

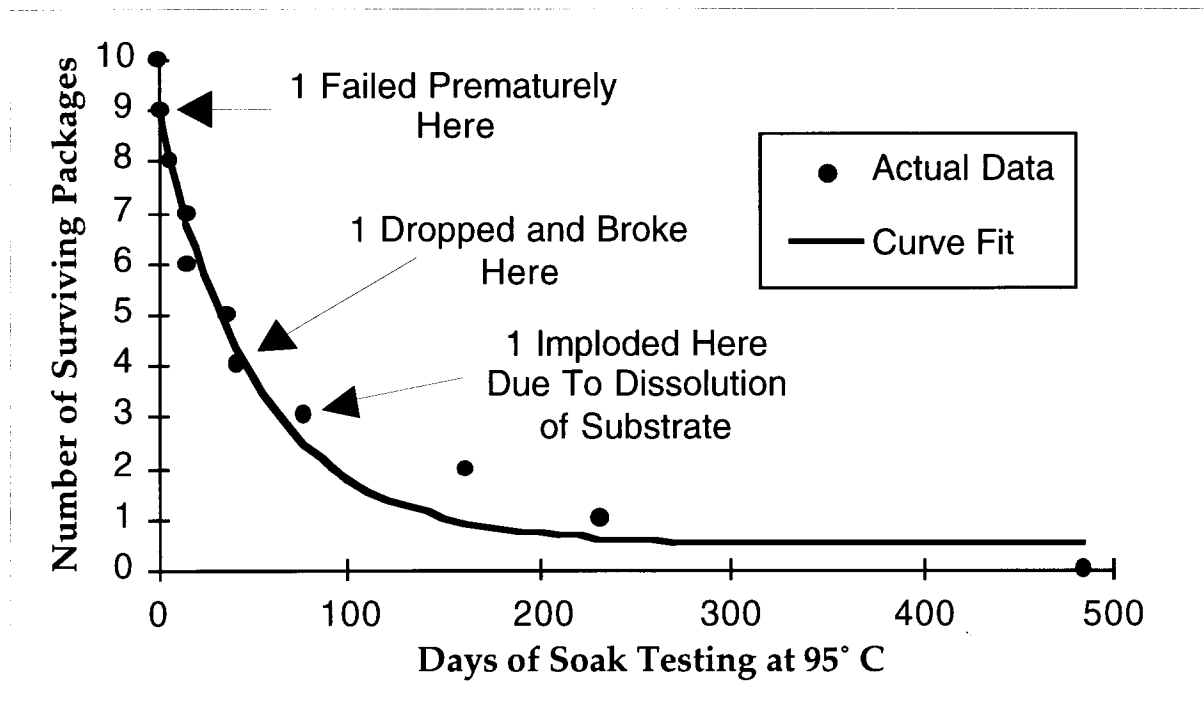


Figure 4: Summary of the lifetimes of the 10 packages which have been soak tested at 95°C in DI water.

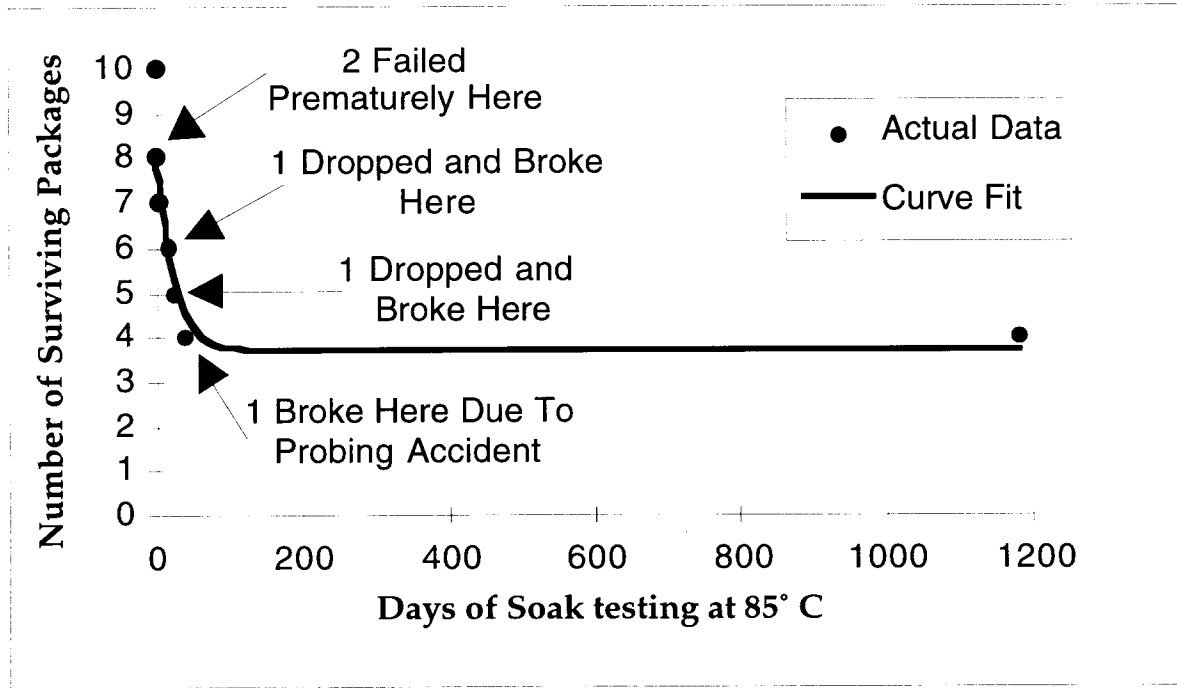


Figure 5: Summary of the lifetimes of the 10 packages which have been soak tested at 85° C in DI water.

2.1.2 Interpretation of the Long Term Soak Testing Results in Deionized Water

Generally during accelerated testing, one models the mean time to failure (MTTF) as an Arrhenius processes (In the VLSI industry this model is used for failure due to diffusion, corrosion, mechanical stress, electromigration, contact failure, dielectric breakdown, and mobile ion/surface inversion). The generalized equation used in all these cases is given below where MTTF is the mean time to failure, A is a constant, ξ is the stress factor other than temperature, (such as pressure or relative humidity), n is the stress dependence, Q is the activation energy, K_B is Boltzman's constant, and T is the temperature in Kelvin.

$$MTTF = A \cdot \xi^{-n} \cdot e^{\left(\frac{Q}{K_B T}\right)}$$

For the accelerated soak tests that we have performed on the packages, there was no stressing factor other than temperature, so the ξ term drops out of the above equation. The resulting equation can be rewritten as a ratio of MTTFs as it is below. This is the model we are using to interpret the accelerated soak tests performed during the past year.

$$AF = \frac{MTTF_{Normal}}{MTTF_{Accelerated}} = e^{\frac{Q}{K_B} \left(\frac{1}{T_{Normal}} - \frac{1}{T_{Accelerated}} \right)}$$

By using these MTTFs at 85°C and 95°C, we can easily calculate the activation energy (Q) and from this activation energy we can proceed to obtain an acceleration factor (AF) for these tests, and then calculate the MTTF at the body temperature. Moreover, after analyzing our failed samples we have found out and mentioned in the past progress reports that some of the samples at the 95°C tests have failed prematurely due to the enhanced dissolution rate for silicon at this temperature. Since the dissolution reaction is an exponential function of temperature, the samples at the 85°C tests have been effected less than the ones at 95°C. The model we use only accounts for acceleration of moisture diffusion, but not dissolution. We will still keep and update the data for the tests performed at 85°C. Moreover, for our calculations we assume that all the samples in the 85°C tests have also failed the same time as the longest going sample in the 95°C tests and proceed with the calculations as follows:

$$MTTF|_{85^{\circ}C} = 257.6 Days \quad MTTF|_{95^{\circ}C} = 118.7 Days$$

$$Q=0.88 \text{ eV}, AF(95^{\circ}C)=179.5, AF(85^{\circ}C)=82.7$$

$$MTTF|_{37^{\circ}C} = 58.4 Years$$

We should also note that we have included every single sample in the 85°C and 95°C soak tests in this calculation except the 15% which failed during the first day (we assume that these early failures can be screened for). Moreover, some of these capsules have failed due to mishandling during testing rather than due to actual leakage into the package. If we disregard the samples that we have attributed failure due to mishandling we obtain a longer mean time to failure:

$$MTTF|_{85^{\circ}C} = 396 Days \quad MTTF|_{95^{\circ}C} = 136 Days$$

$$Q=1.217 \text{ eV}, AF(95^{\circ}C)=1304, AF(85^{\circ}C)=447$$

$$MTTF|_{37^{\circ}C} = 485 Years$$

2.1.3 Accelerated Soak Tests in Phosphate Buffered Saline With Silicone Coated Glass Silicon Packages

We have continued our accelerated soak tests with the ultrasonically machined glass capsules bonded to silicon substrates. In these tests, after bonding we have coated the interface between the glass capsule and the polysilicon bond with a biocompatible silicone-coating to prevent the dissolution of the polysilicon. Tables 4 and 5 below give an update of the summary for these devices. Figure 6 summarizes the soak tests at 95°C in saline solution.

We have started with 8 devices each at 85°C and 95°C. Out of the original 8 packages in the 85°C tests, one of them failed after one day (premature failure) due to a fault on the bonding surface. The remaining 7 are still dry and being tested. Some dissolution is observed around the edges of the devices (some of the testing pads have been eroding away and hence preventing us from electrically testing some of the dew point sensors). However, the silicone coating is

effectively preventing the corrosion of polysilicon in any of the samples tested at this temperature. Moreover, out of the original 8 packages in the 95°C tests, we have one device that has failed after one day (sample is excluded from calculations) due to a scratch on the polysilicon bonding surface and we still have 3 that are under testing. We have analyzed the samples that have failed which will be detailed in a following failure analysis section.

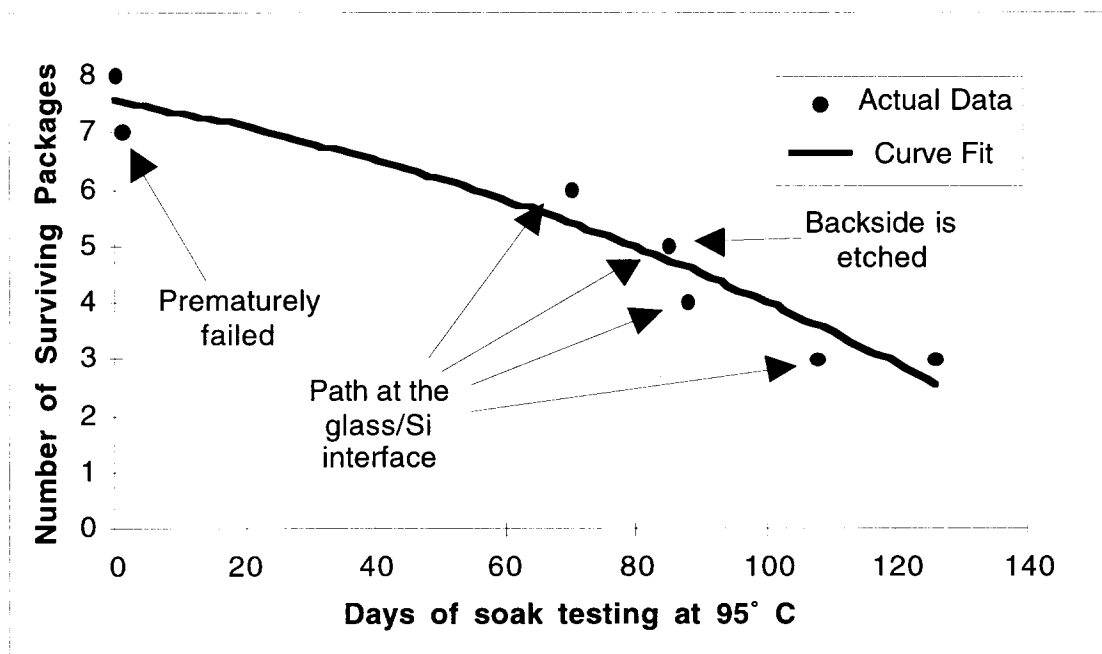


Figure 6: Summary of the lifetime of the 8 packages soaked in saline at 95°C.

For the tests at 95°C, assuming that the remaining 3 samples fail today, we can proceed and calculate a worst case Mean Time to Failure (MTTF) of 104 days. If we compare these results with the ones for the uncoated devices, in which the MTTF at 95°C was only 38 days, we see that with the silicone coating we have been able to slow the dissolution mechanism significantly. We cannot calculate the activation energy (Q) from the present results due to insufficient data, but using the Q derived from the tests of the uncoated devices in saline at 95°C, and assuming an MTTF of 104 days at this temperature, we get a MTTF at body temperature of 482 years for the coated packages. This result will be confirmed and updated as the current tests conclude.

The packages in these accelerated tests have been monitored every few days for room temperature condensation both electrically by means of an integrated dew point sensor and also visually with the aid of a microscope. We define failure as room temperature condensation. With these ultrasonically machined glass capsules, due to their flat top surface, we have the additional advantage of being able to monitor their bonding surface and the glass capsule to polysilicon interface for discoloration and dissolution. We have found that even though the saline solution is refreshed daily to maintain a constant concentration, at these high temperatures without a silicone coating it is simply very hard to prevent the dissolution of the polysilicon layer. We are looking into other ways to inhibit polysilicon dissolution at these high temperatures. We are considering using teflon as a barrier against the high temperature tests. For this purpose, we have prepared 5 packages and sent them to Dr. Edell at MIT for teflon coating during this past quarter. After we receive the devices, we will start a new set of tests to see whether the teflon coating is effective for our application.

Table 4: Key data for soak tests in saline at 85°C.

Number of packages in this study	8
Soaking solution	Saline
Failed within 24 hours (not included in MTF)	1
Longest lasting packages in this study	126 days
Packages still under tests with no measurable room temperature condensation inside	7
<i>Average lifetime to date (MTTF)</i>	<i>126 days</i>

Table 5: Key data for soak tests in saline at 95° C.

Number of packages in this study	8
Soaking solution	Saline
Failed within 24 hours (not included in MTF)	1
Longest lasting packages in this study	126 days
Packages still under tests with no measurable room temperature condensation inside	3
<i>Average lifetime to date (MTTF)</i>	<i>104.1 days</i>

2.1.4 Failure Modes

The devices in these tests have been checked for moisture penetration every few days both with the dew point sensors and also visually with the aid of a microscope. The possible failure mechanisms are outlined in the Figure 7 below.

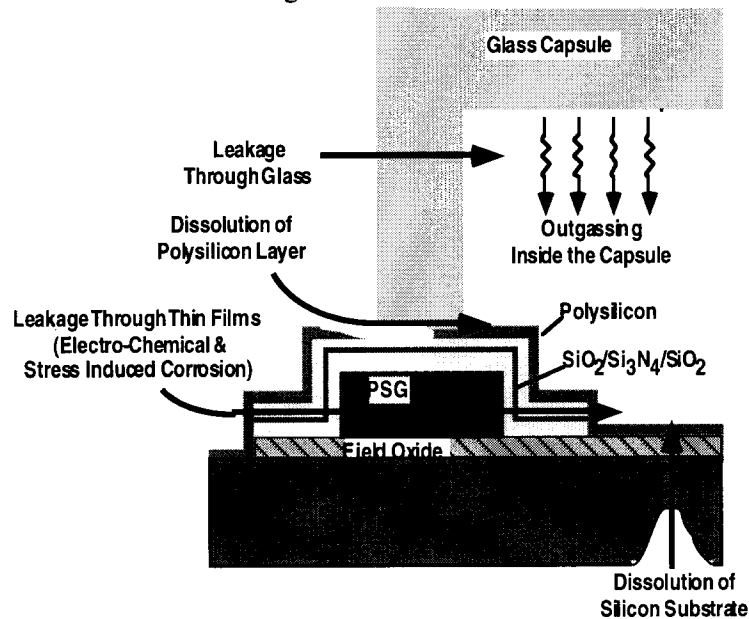


Figure 7: The possible failure modes for the microstimulator package.

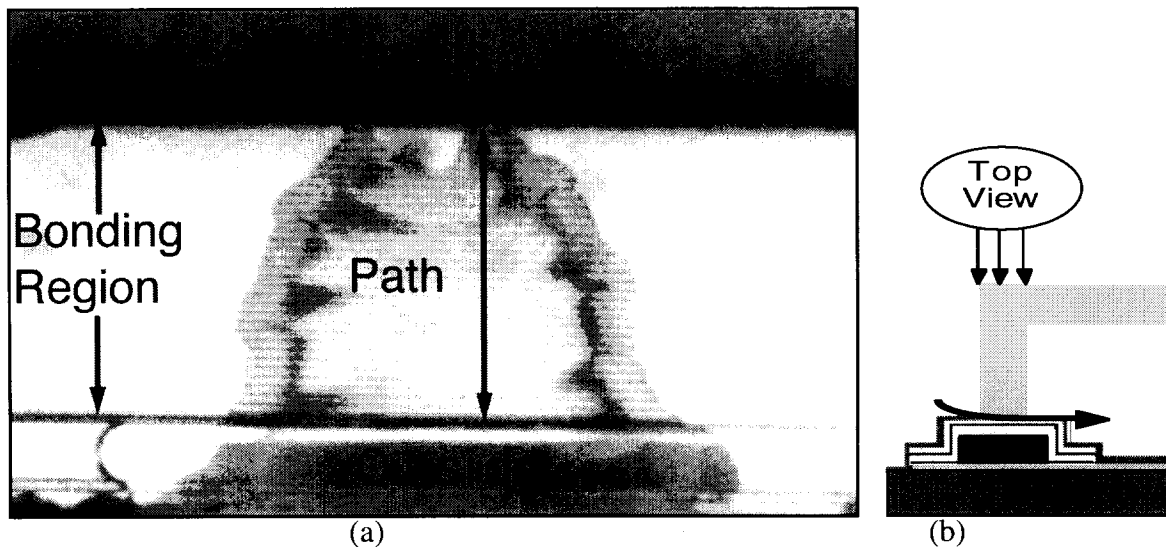


Figure 8: Leakage path through the interface between glass and silicon seen from top after soaking for 88 days at 95°C.

The main failure mode observed on the packages that have failed during this last quarter is similar to the ones described in our earlier progress reports in which the failures are attributed to the dissolution of a polysilicon layer just below the glass capsule. The dissolution of the polysilicon layer eventually creates a path, a typical one of which can be seen on Figure 8(a). Figure 8(b) shows the way the picture is taken from the top.

Another possible failure mode has been identified, which is the dissolution from the backside of the silicon substrate. However, it seems that the oxide layer is not significantly affected by this dissolution and thus prevents or slows dissolution from penetrating inside the package. Indeed, we have not been able to surely identify any device that failed with this kind of failure because the usual failure mode (path through the interface between the glass capsule and the silicon substrate) has always occurred first or almost simultaneously. Figure 9(a) shows a picture of the backside of the device etched to the point that we can see the inside of the package (region A shows dissolution of the backside of the substrate and of the glass/silicon interface, region B shows dissolution of the backside of the substrate only and region C shows the remaining non etched layers). Figure 9(b) shows the way the picture is taken from the top. We will continue to monitor the backside of the package as well as the bonding surface while looking for failures.

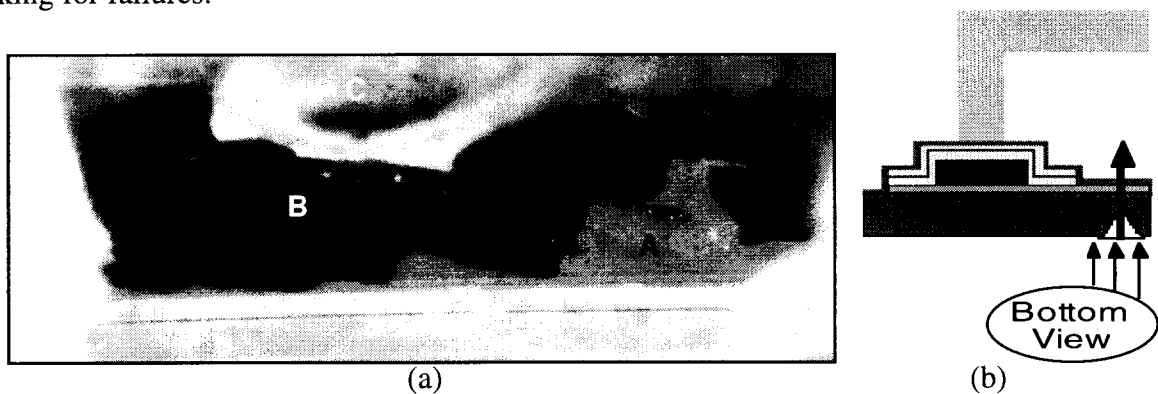


Figure 9: Backside view of the device.

2.1.5 Ongoing Room Temperature Soak Tests in Saline

We have continued the soak tests of packages at room temperature in phosphate buffered saline solution. Table 6 below summarizes the pertinent data from these soak tests. We originally started these soak tests to complement the accelerated soak tests at the higher temperatures. We have consistently observed in these tests that at room temperature we are below the activation energy required to cause dissolution and hence as of yet have not observed any dissolution related failures.

We have soaked 6 packages in phosphate buffered saline at room temperature. One of these packages leaked within a day, indicating surface defects or poor alignment of the glass capsule to the silicon substrate. Another one failed after 160 days of soaking. The longest lasting package has survived a total of 1090 days and is still under test. The remaining 4 packages have shown no sign of moisture either measured electrically or observed visually after an average of 897 days of soaking and are still under test.

Table 6: Data for room temperature soak tests in saline.

Number of packages in this study	6
Soaking solution	Saline
Failed within 24 hours (not included in MTTF)	1
Packages lost due to mishandling	1
Longest lasting packages in this study	1090 days
Packages still under tests with no measurable room temperature condensation inside	4
<i>Average lifetime to date (MTTF)</i>	<i>896.8 days</i>

2.1.6 In-Vivo Tests

During this quarter we have continued our activities in performing the biocompatibility studies of our the glass silicon package in animal models. We had started 3 implants in the dura of a Guinea Pig during a previous quarter at the Kresge Hearing Institute at the University of Michigan. This quarter the final one of these devices was harvested after 2 months. After harvesting, this device came out intact and also the dew point sensors and the visual inspection indicate that the device remained hermetic during the duration of the implant. Figure 10 shows the implanted device after 2 months of implantation residing on top of the dura of a Guinea Pig just before explantation. The histology study for this device is underway and will be reported as results become available. We have next prepared 8 more devices for Prof. Zealea at Vanderbilt University. These devices are being shipped to him and will be implanted shortly. The implants that were started at the Hines VA Hospital in Illinois under the supervision of Dr. Reidy are in progress and the results will be reported soon.

2.1.7 Characterization Of An All Silicon Package

We have fabricated an all Silicon package with the use of an intermediate layer of evaporated glass in the previous quarter. With this technology we are planning on utilizing the tools and processes that are well characterized for Silicon processing technology and can make packages in house with different dimensions and shapes at a very low cost. Using this technology in the past had been somewhat problematic due to the slow deposition rate of

sputtered glass. With the progress in the quality and rate of deposition of the evaporated glass layers, one can deposit glass layers of required composition at a rate of 1 micron/minute. The prototype package as seen in Figure 11 is fabricated by anodic bonding of a regular microstimulator substrate and evaporated glass deposited silicon wafer. This package is diced along the dashed lines and an SEM micrograph is taken to show the interface of the bond. The cross section of this device (Figure 12) shows the layers in this package. In order to fabricate this device, a 5 micron thick glass is first evaporated on a Silicon wafer which is flipped over and bonded to a regular microstimulator substrate. As such the bond is achieved between evaporated glass which was on a silicon wafer and the thin polysilicon film on the microstimulator substrate. We have experimented with different film thicknesses ranging from 5 to 10 microns and also temperature during bonding which varied from 320°C to 370°C. Due to the thin layer of evaporate glass, the maximum applied voltage for anodic bonding is limited to about 500 Volts. We next have proceeded to characterize the strength of these bonds.

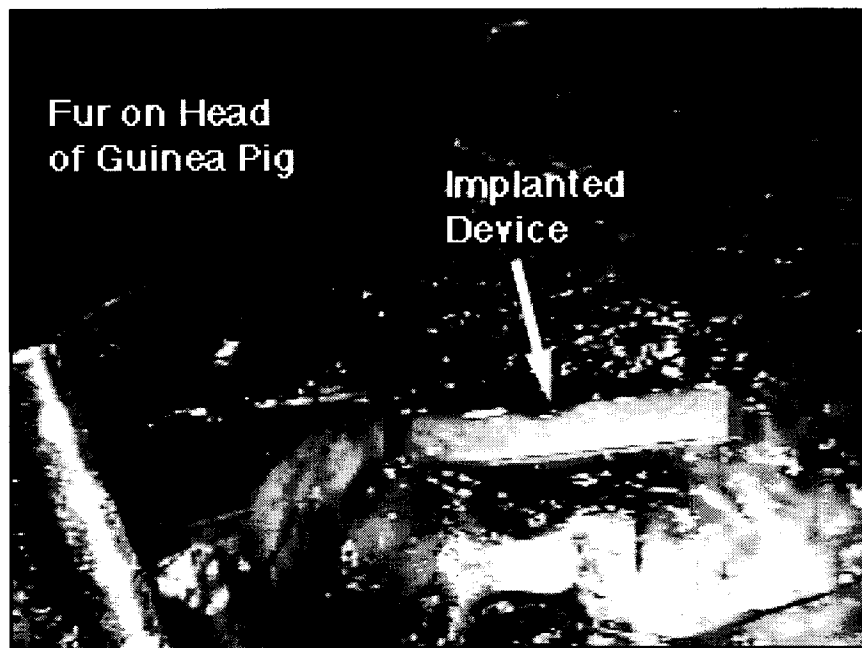


Figure 10 : The picture of the implanted device residing on the top of the dura of a Guinea Pig.

During this quarter we have made 9 of these bonds and have pulled them apart. Figure 13 shows the outcome of the results obtained so far from these tests. The broken pieces have been examined under both a optical microscope and a SEM, both of which indicated the presence of a strong bond between the evaporated glass and polysilicon. The analysis of the pulled devices shows that in most places the evaporated glass film has been peeled off while pulling the device apart. In some cases, we have seen the presence of thin films from the microstimulator substrate coming out. In both cases, the actual bond between the polysilicon layer and the evaporated glass remained intact. Table 7 below shows a comparison between the bonds made to bulk Pyrex glass which was 2.3 mm thick and evaporated glass with a thickness of 10 microns. The results of these pull tests indicate that the bonds are of similar quality of the bonds made to bulk Pyrex glass capsules. We are very excited about these preliminary but promising results and hope to continue our effort using this technology and will fabricate more devices in the future. As can be seen from Fig. 13, there is still a considerable variation in the strength of these bonds and this is an issue which requires further optimization of the bond conditions.

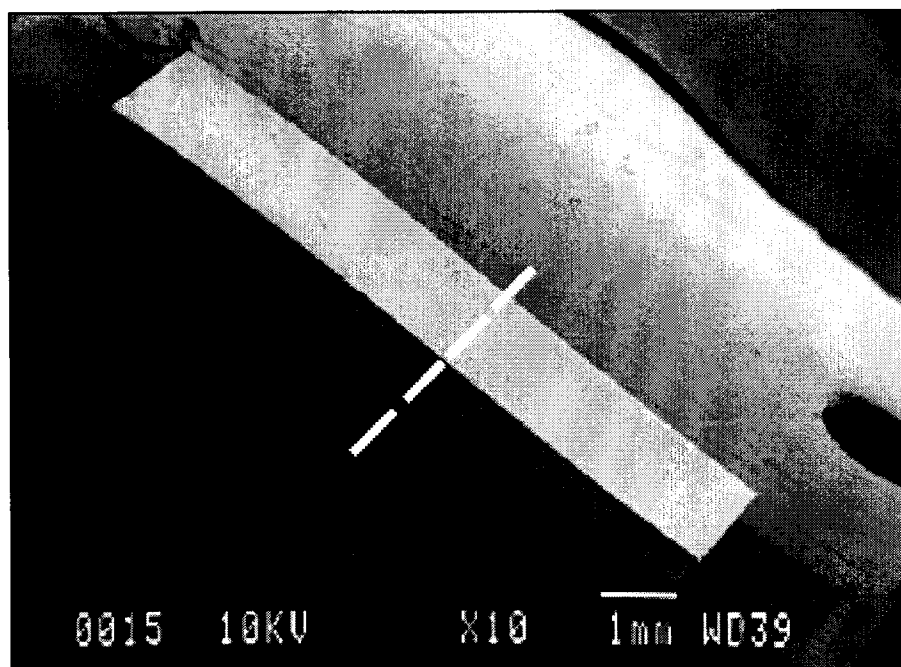


Figure 11: The SEM micrograph of the all silicon package made with evaporated glass deposited on silicon bonded to a microstimulator packaging substrate.

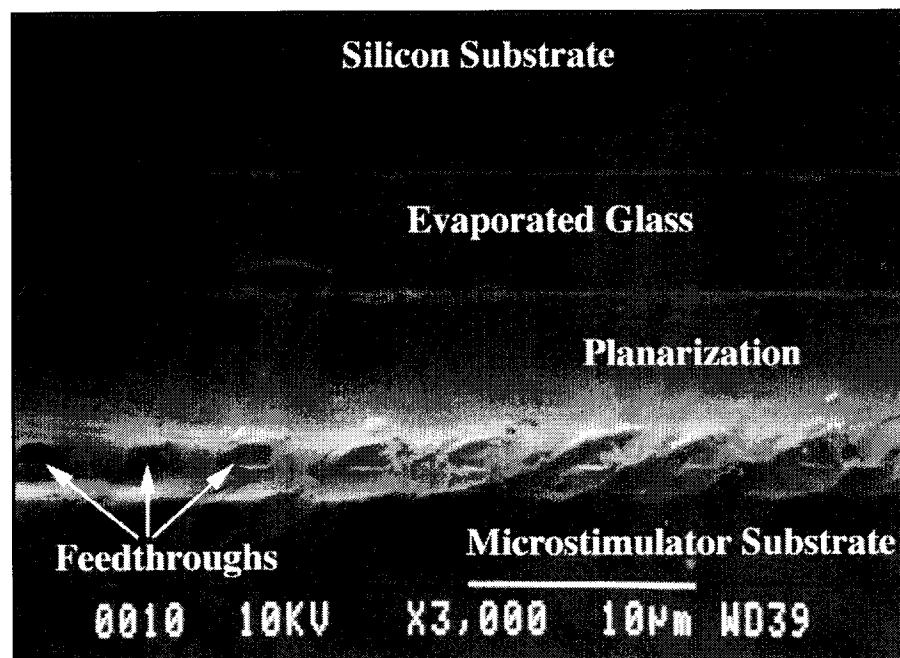


Figure 12: The close up view of the bond between polysilicon and the evaporated glass.

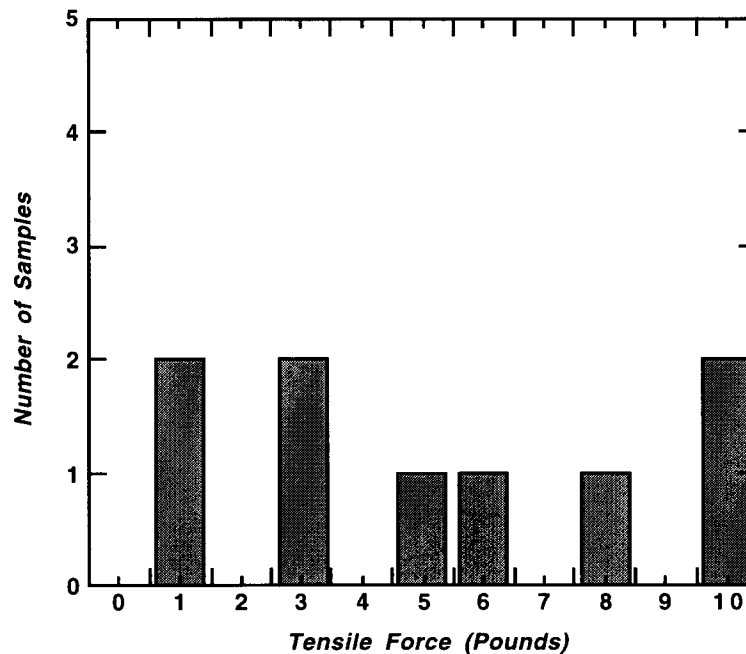


Figure 13: The summary of pull test results from polysilicon to evaporated glass.

Table 7: Comparison of pull test results between polysilicon and evaporated glass and bulk pyrex glass.

Parameter	Bulk Glass Bond	Evaporated Glass Bond
Number of Samples	14	9
Average (Pounds)	6.6	5.1
Maximum (Pounds)	13.5	9.75
Standard Deviation	1.95	3.6

2.2 Circuit Fabrication and Test Results

This quarter we fabricated a new batch of wafers containing the single channel microstimulator, the multichannel microstimulator, and the peripheral nerve stimulation system. So far we have tested two of the systems on the new batch of wafers; the single channel microstimulator and the 8-channel peripheral nerve stimulation system, and both work as expected. We now have ample working single channel microstimulator circuits which take less power than any of our previous designs. We also have ample working peripheral nerve stimulation circuitry. These circuits have to be tested via telemetry, which will be conducted in the coming quarter. These early results are clearly very encouraging as we will discuss below.

The single channel microstimulator has worked on previous fabrication runs, but it always consumed more power than we expected. The circuit was redesigned this summer to consume about 1/3 less power. The stimulating output current source was also redesigned to be better regulated and to have an adjustable amplitude. This redesigned circuitry was fabricated this quarter and our testing shows that it works nicely.

The peripheral nerve stimulation system is designed to be fully integrated with an on-chip coil, and as a result it will be almost an order of magnitude smaller in volume than the microstimulator when both systems are completely assembled (as shown in Figure 14). We call the peripheral nerve stimulation circuit FINESS (Fully Integrated Nerve Electrical Stimulation System). The FINESS circuitry has been tested and is completely working, however on-chip coils have not yet been integrated on top of the circuitry. We will integrate coils with this circuitry during the coming quarter, and will report on complete telemetry results in the final report.

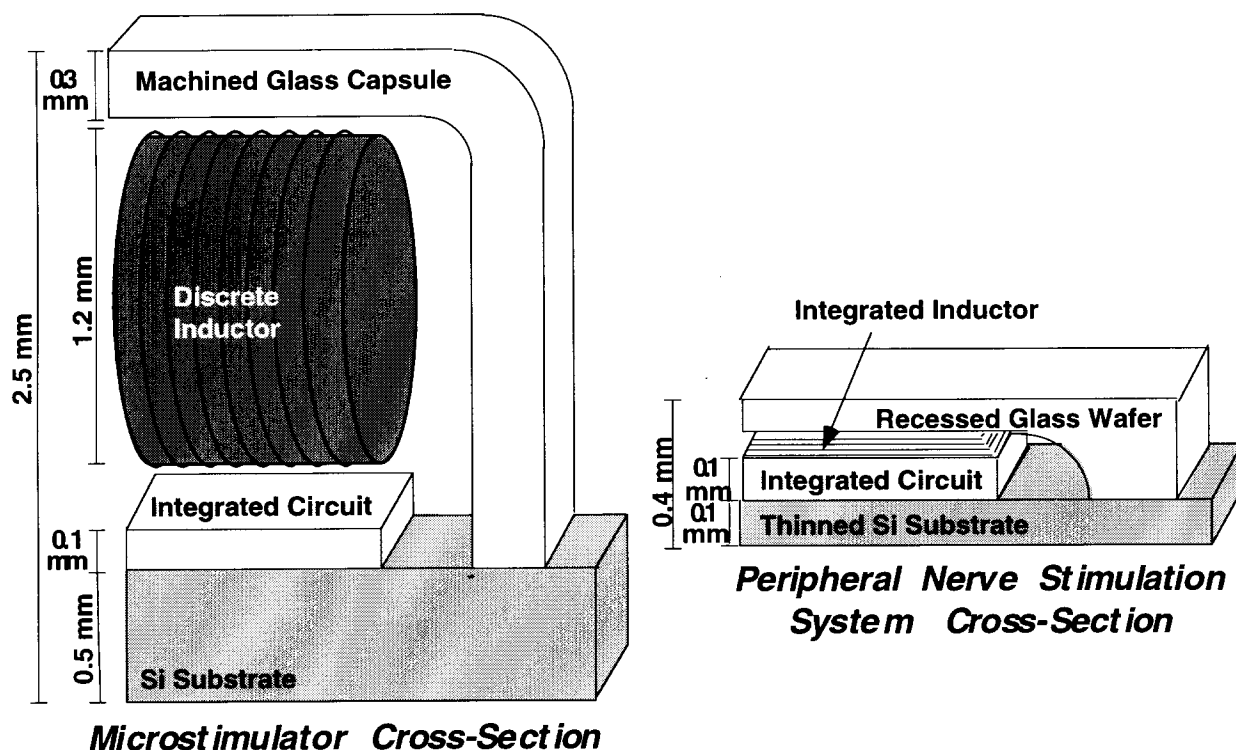


Figure 14: A scale drawing comparing the volume of the microstimulator with the volume of the FINESS chip.

2.2.1 Test result from the Single Channel Microstimulator

Table 8 shows the specifications for the single channel microstimulator, and Figure 15 shows the stimulating output of a microstimulator from this latest fabrication run. The stimulating output of the microstimulator in Figure 15 has been set to 8 mA (this is done by laser trimming). It is shown delivering a 200 μ s stimulation pulse to a 1 k Ω load. The power requirement of the microstimulator circuitry has successfully been reduced by a factor of 1/3 from our earlier designs. Microstimulators from our earlier fabrication runs consumed a current of about 3 mA. The current consumption of the microstimulators that we fabricated this quarter is 1.6 mA DC during very low frequency stimulation, and about 1.9 mA during 40 Hz stimulation. This power reduction was achieved by reducing parasitic junction leakage and by reducing the bias currents in several of the internal circuit blocks. Note that the stimulating output and reliability of the microstimulator has not been affected in any way by the redesign. The microstimulator is still capable of delivering 2 μ C of charge in 200 μ s pulses at 40 Hz.

Table 8: Single channel microstimulator specifications.

General	
Device Dimensions = 2.0 mm X 2 mm 10 mm	Power Delivery = Telemetry
Power Consumption < 20 mW	On-Chip Regulated Supply = 8V, 4V, Gnd
Biocompatible Hermetic packaging Operational In-Vivo for Ten Years @ 37 °C	
High Current Thin Film Micro-electrodes Capable of delivering 2 μ C of charge	
Telemetry Link	
Receiver Coil = On-chip (2.0 mm X 8.0 mm)	Carrier Frequency = 2 MHz
Transmitter Coil = solenoid, air core (9 cm dia.)	Modulation Frequency = 2 kHz to 10 kHz
Modulation = ASK, Pulse width encoded	
Range = Anywhere inside 9 cm diameter transmitter coil	
Device Addressability = up to 32 individually addressable devices per transmitter	
Stimulation	
Stimulation waveform = 10 mA stimulating pulse followed by 100 μ A charge balancing pulse	
Duration (stimulating phase) = up to 200 μ s	Output Channels = 1
Stimulation Frequency \leq 40 Hz	Maximum Output Load = 800 Ω

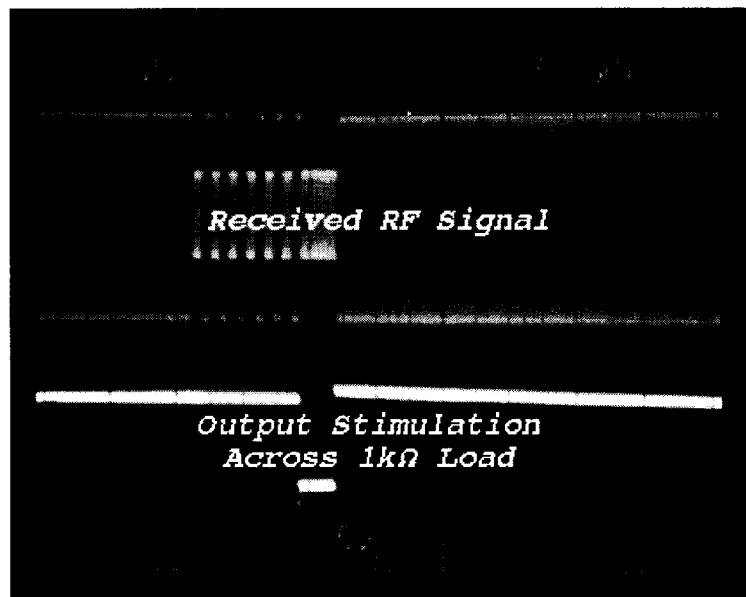


Figure 15: The stimulating output of the microstimulator across a 1 k Ω load. The amplitude of the stimulating output for this device has been set to 8 mA.

2.2.2 Test result from the FINESS chip

The FINESS chip was fabricated and tested and found to work perfectly. Figure 16 is a photograph of a die of the fabricated and fully functional FINESS circuitry. The FINESS system design differs from the microstimulator in two major ways (both of which make the FINESS system much smaller than the microstimulator). First, it has an integrated RF telemetry coil for receiving power, while the microstimulator has a discrete telemetry coil. We have not yet electroplated the on-chip coil on the FINESS circuitry. Second the FINESS circuit has no charge storage capacitor, while the microstimulator has a large discrete charge storage capacitor. Because the FINESS system does not have a charge storage capacitor, its output stimulating

current magnitude is limited to about 2 mA. Table 9 reviews the specifications for the FINESS chip, and Table 10 reviews the 45 data bits that need to be telemetrically sent in order to program the FINESS chip for a stimulation.

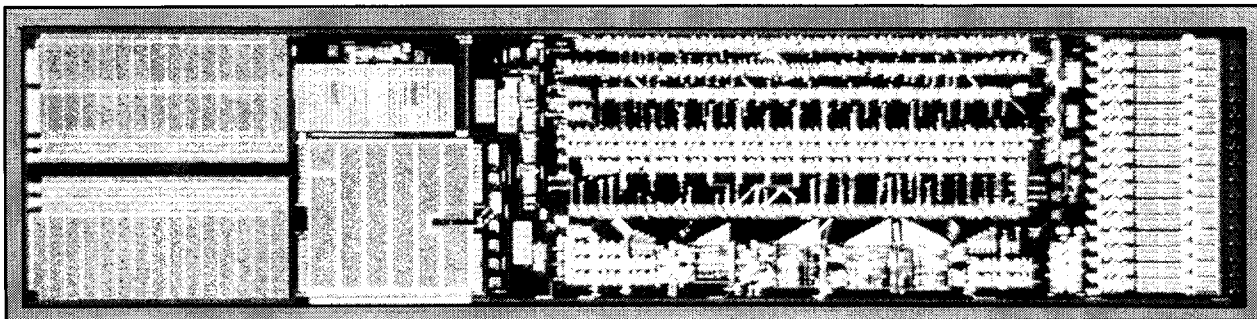


Figure 16: A photograph of the fabricated FINESS circuitry.

Table 9: FINESS specifications.

General	
Circuit Area = 2.0 mm X 8.5 mm	Power Delivery = Telemetry
Power Consumption < 12 mW	On-Chip Regulated Supply = 4 Volts, Gnd
Telemetry Link	
Receiver Coil = On-chip (2.0 mm X 8.0 mm)	Range (coil to coil distance of link) = 3 cm
Transmitter Coil = Planar, air core (80 mm dia.)	Carrier Frequency = 4 MHz
Modulation Frequency = 1 kHz to 50 kHz	Modulation = ASK, Pulse width encoded
Device Addressability = up to 8 individually addressable devices per transmitter	
Stimulation	
Stimulation waveform = Two independent phases of opposite polarity	
Amplitude = 0 to 2 mA (64.5 μ A steps), each phase independently programmable	
Duration (each phase) = 4 to 2050 μ s (2 μ s steps), each phase independently programmable	
Output Channels = 8 (supports 16 electrode pairs)	Inter-phase delay = 12 to 1932 μ s (16 steps)
Stimulation Frequency \leq 50 Hz	Maximum Output Load = 1.5 K Ω

Table 10: The 45 data bits which are transmitted for each stimulation

Parameter	Range	Required Bits
Address of Device	Selection from up to 8 devices	3 bits
1st Phase Current Magnitude	0 to 2 mA (32 steps of 64.5 μ A)	5 bits
2nd Phase Current Magnitude	0 to 2 mA (32 steps of 64.5 μ A)	5 bits
Electrode Selection	Selection from 8 electrodes pairs	3 bits
1st Phase Duration	4 to 2050 μ s (1024 steps of 2 μ s)	10 bits
Inter-phase Delay	12 to 1932 μ s (16 steps of 128 μ s)	4 bits
2nd Phase Duration	4 to 2050 μ s (1024 steps of 2 μ s)	10 bits
Parity Bits		5 bits
Total		45 bits

2V 10

Received AM RF Signal

22

Many different combinations of programmed stimulation phase amplitudes, stimulation phase durations, electrode pair selections, and inter-phase delays were tested, and in every case the FINESS chip did exactly what it was supposed to do. Figure 19 shows the output of the FINESS chip when the RF received signal is exactly the same as in Figure 17, except for a single parity bit which was changed to be wrong. As can be seen, the FINESS chip correctly recognized the bad parity and did not stimulate. In a similar test, a single bit in the device address in the RF signal was changed to be wrong, and again the FINESS chip correctly recognized the bad address and did not stimulate. In a third test, a single bit of data was changed to be inconsistent (the envelope high duration indicated a zero bit, and the envelope low duration indicated a one bit) and again the chip correctly recognized the inconsistent data and did not stimulate. Finally, an improperly timed synchronization pulse was sent to the chip, and the chip correctly recognized an error and did not stimulate. In each of these cases, as soon as the error was corrected in the transmitted data stream, the FINESS circuit immediately started stimulating with the exact waveform shown in Figure 17.

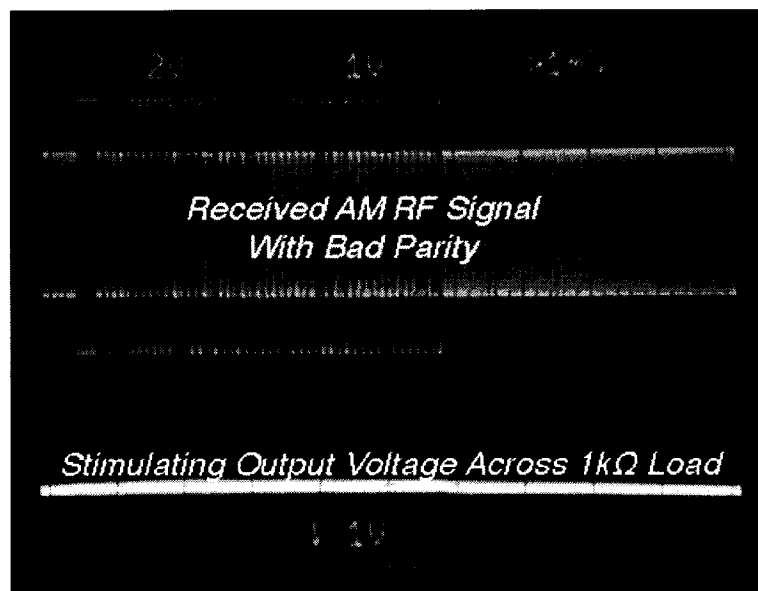


Figure 19: The stimulating output when the telemetry input signal is exactly the same as in Figure 17 except one parity bit has been changed to be invalid. The circuitry correctly recognizes the bad parity bit and does not stimulate.

The system was tested by cycling through many of the possible 45-bit programmed input possibilities (but obviously not all of the input possibilities because there are over 10^{13} of them). Every single one of the dozens of tested input combinations resulted in the logic doing exactly what it was programmed to do. First, the system was programmed to stimulate at many different output pulse durations. The system correctly timed the output pulse duration in every case. The system was then programmed to stimulate each of the eight electrode pairs. In each case, the FINESS chip selected the correct electrode pair. Finally, the system was programmed to stimulate at each of the 32 output stimulation magnitudes, and again in every case the system stimulated at the proper magnitude. ✓

The programmable output current source of the FINESS chip has an amplitude which is 5-bit programmable (32 discrete levels). Figure 20 shows the programmable output current source of the FINESS chip ramping through all 32 discrete stimulation levels. As can be seen,

the response of the output current source is almost perfectly linear with respect to the programmed amplitude. Although the current source was designed to have a full scale amplitude of 2 mA, the actual measured full scale current amplitude is about 2.8 mA. This is due to the transistor threshold values being slightly lower than target. However, there are ample links in the output current source which allow the full scale amplitude to be adjusted by laser cutting. Cutting a few links in the circuit will set the full scale stimulating magnitude to be 2 mA or any other reasonable value.

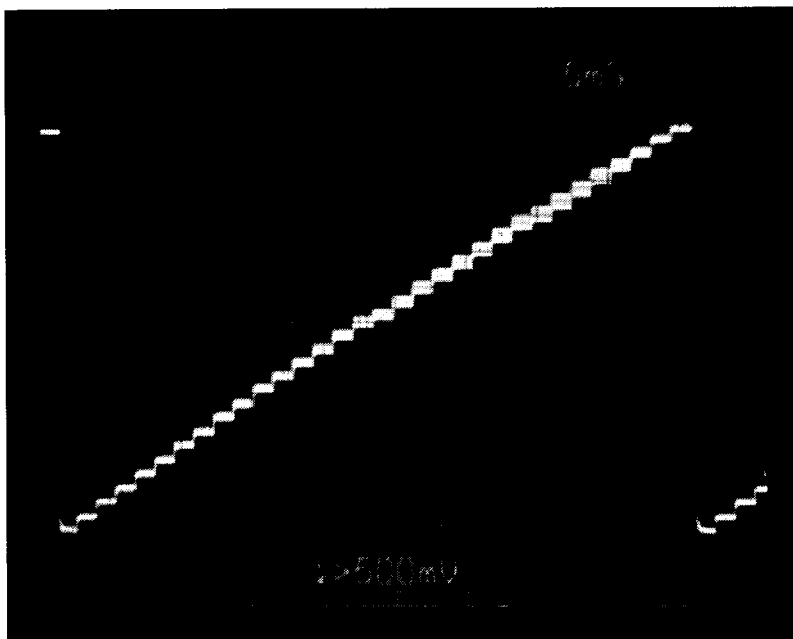


Figure 20: The FINESS chip stimulating output current source ramping through all 32 programmable stimulation levels. The output is shown across a 1.5 k Ω load.

The measured power requirements of the FINESS chip are given in Table 11. The system has a measured non-stimulating current draw of 1.56 mA, during a full scale stimulating output of 2 mA, the current draw is 3.6 mA. Measurement with on-chip coils show that we should not have any problems supply this amount of power over link distances of at least couple of centimeters.

Table 11: The measured power requirements of the FINESS chip.

Measured Parameter	Average	Standard Deviation
DC current (non-stimulating)	1.56 mA	0.08 mA
Minimum voltage needing to be received	6.78 V	0.027 V
Minimum power requirement	10.57 mW	0.6 mW

- Power
10 mW

2.3 On-Chip Coil Measurements

The high efficiency on-chip coils which will be used to inductively power the FINESSE circuit were tested this quarter by putting them in an actual telemetry link, and measuring the power they received. Previously we have reported telemetry test results from less efficient on-chip coil designs, but this quarter is the first time that we have telemetrically tested our most efficient coils. These coils are 17-turn coils with an electroplated NiFe core located underneath the electroplated Cu windings. The structure of these coils is shown in Figure 21.

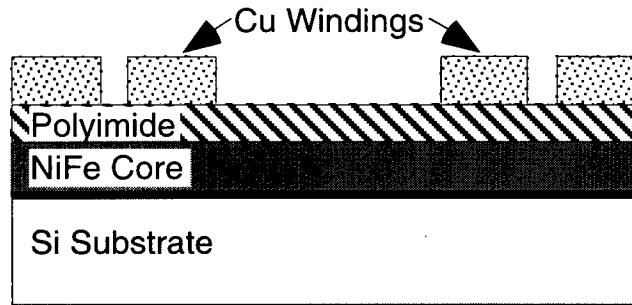


Figure 21: The structure of the on-chip coils tested this quarter

Figure 22 is a photograph of the testing setup for measuring the power received by the on-chip coils. A class-E transmitter was used to drive a 16-turn, 25 μ H planar spiral transmitter coil with average winding diameter of 8 cm. The class-E was powered by a 4.5 V DC supply, and it delivered a 200 V amplitude sinusoidal signal to the transmitter coil at 4 MHz. We would like to have had the class-E run off a 9 volt supply for these measurements, however this class-E was originally designed and built to work at 2 MHz for powering the microstimulator and this particular class-E does not operate as efficiently at 4 MHz. It was found that when tuned to 4 MHz, components in this class-E would overheat and burn out if more than about 4.5 V was supplied to then. With a class-E specifically designed to operate at 4 MHz, a 9 V supply can be used, and the transmitted power would be much greater.

All of the test results reported on in this section were obtained with 17-turn on-chip receiver coils of the structure shown in Figure 21. The on-chip coils were prepared by attaching them to a small printed circuit board by wire bonds. The printed circuit board has sockets for a parallel capacitor to be added to tune the coil to resonate at 4 MHz, and for a parallel resistive load to be added. By exciting the on-chip coil inductively with the transmitter, and recording the resulting peak voltage across the load, the power delivered to the load can be easily calculated. Many applications for these on-chip coils (including the FINESSE system), require the received inductively coupled AC signal to be converted to a DC supply voltage. In these systems it is the DC power delivered to a DC load after rectification of the received signal that is of importance, not the AC power delivered to an AC load. However, in order to keep the measurement setup simple, the peak AC power delivered to an AC load without rectification was recorded in these experiments. The AC load was converted to an equivalent DC load by Equation 1, and the peak AC peak power delivered to the AC load was converted to the equivalent DC power delivered by Equation 2.

$$AC\ Load = \frac{1}{2} DC\ Load \quad \text{Equation 1}$$

$$AC\ Peak\ Power = 2\ DC\ Power \quad \text{Equation 2}$$

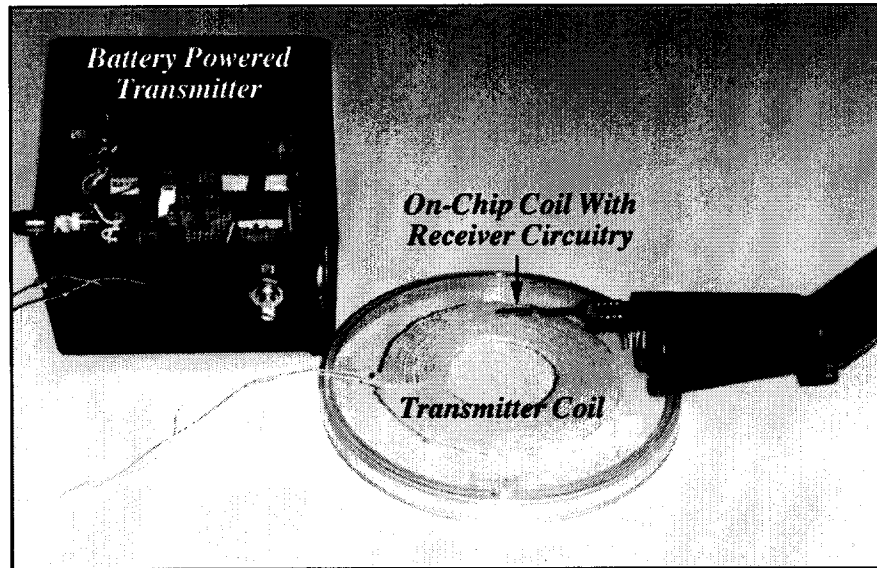


Figure 22: The testing setup used to measure the power received by the on-chip coils in an inductively coupled link.

The measured DC power received with an on-chip coil as a function of link distance is given in Figure 23. These measurements were made with a $2\text{k}\Omega$ equivalent DC load (this correctly models the 2.7 mA maximum current draw of the FINESS chip at about 5.5 volts peak received). As can be seen, the 15 mW maximum power required by the FINESS chip can be received at a link distance of 2 cm even with the inefficient class-E transmitter running with only half of the target supply voltage. Figure 23 includes a calculated curve showing the expected received voltage under these conditions according to the model that we have developed. As can be seen, the measurements closely agrees with the modeled results.

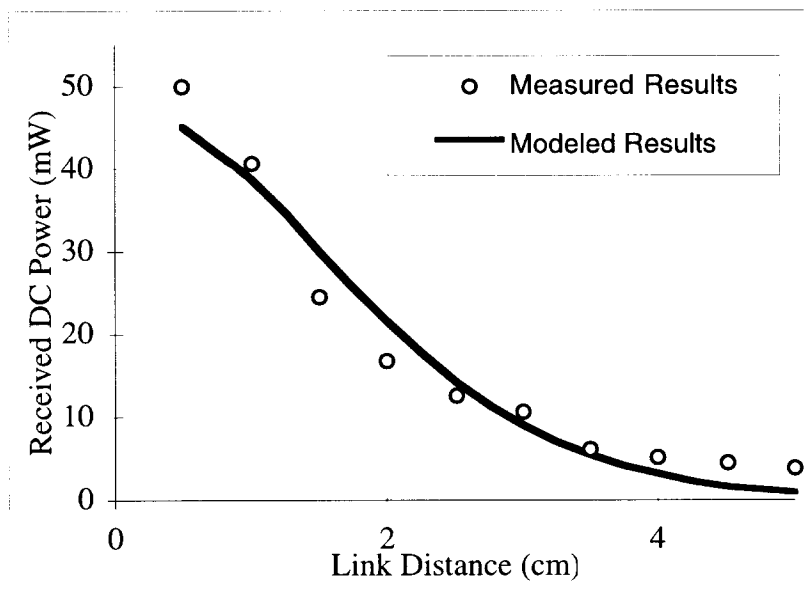


Figure 23: Measured DC power received as a function of link distance for a 17-turn, 2 by 10 mm on-chip receiver coil with a $2\text{k}\Omega$ load, when powered by a 4 MHz class E transmitter with a 4.5 V supply.

The measured DC power received as a function of DC load resistance is given in Figure 24. These measurements were made at a link distance of 1 cm, with a 17-turn on-chip receiver coil. Also shown in Figure 24 is the expected power received under these conditions. Again it can be seen that the modeled behavior of these coils closely match actual measurements.

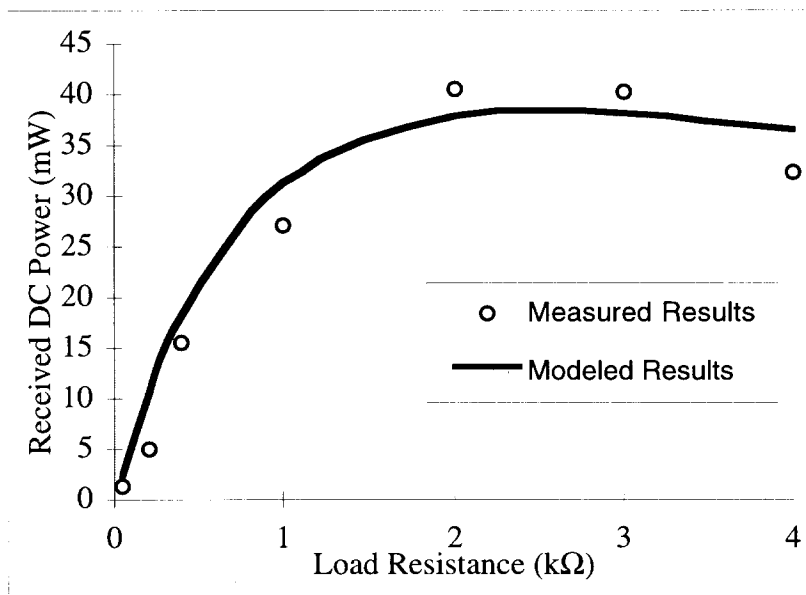


Figure 24: Measured DC power received as a function of load resistance for a 17-turn, 2 by 10 mm on-chip receiver coil at 1 cm link distance, when powered by a 4 MHz class-E transmitter with a 4.5 V supply.

Figure 25 shows the measured power received as a function of the axial misalignment of the coils at a link distance of 1 cm. Also shown in Figure 25 is radius of the transmitter coil. Since the transmitter coil is 8 cm diameter, an axial misalignment of 4 cm means that the relatively small on-chip coil is located right at the edge of the large transmitter coil. As can be seen in the Figure, a large coil misalignment of up to 2 cm in any direction can be tolerated by this inductively coupled link with almost no degradation in performance. This is important in functional electrical stimulation applications where the transmitter coil will most likely be applied and removed from the skin frequently, without careful alignment. It also means that multiple microsystems spread out over a 12.6 cm² area (a circle with 2 cm radius) can be powered by a single 8 cm transmitter coil.

3. ACTIVITIES PLANNED FOR THE COMING QUARTER

Our efforts on the various aspects of this project will continue in the coming quarter. First, we will continue soak tests of glass-silicon packages in saline and will acquire additional soak test data to complement that we obtained previously. Testing of the new set of glass capsules that have been coated with silicone will continue to further study the effect of dissolution at these higher temperatures. We will continue to develop techniques for preventing the dissolution of polysilicon at higher temperatures so that long-term accelerated tests could continue to be conducted.

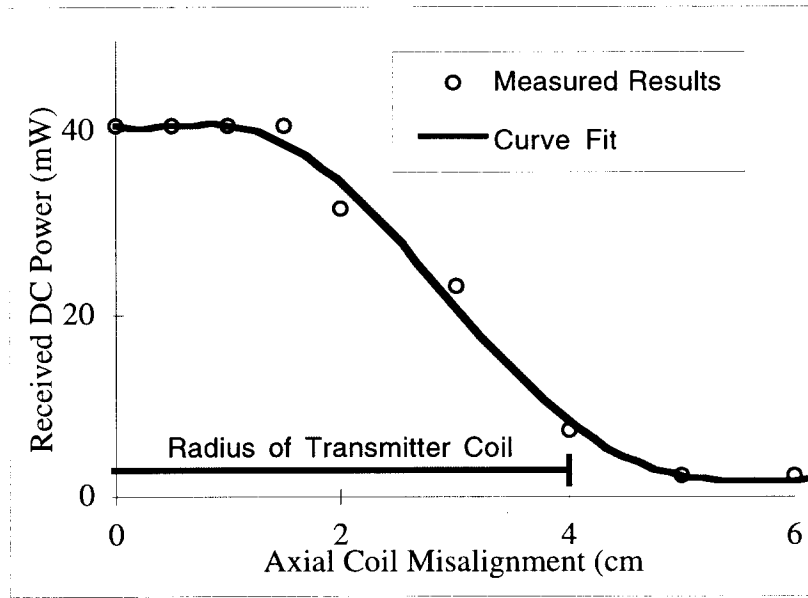


Figure 25: Measured DC power received as a function of axial coil misalignment for a 17-turn, 2 by 10 mm on-chip receiver coil with 2 k Ω load at 1 cm link distance, when powered by a 4 MHz class-E transmitter with a 4.5 V supply.

In the area of microstimulator development, in the coming quarter we will continue to test the microstimulator using telemetry and also will assemble several units for in-vitro and in-vivo testing. In addition, the FINESSE chip will undergo further testing using the on-chip integrated coil which is now in fabrication.

Finally, we will continue to work with a number of groups that have been interested both in microstimulators and in our packaging technology, including Vanderbilt University, VA Hines Hospital, Case Western Reserve University, Johns Hopkins University. Results from these collaborations will be reported as they become available.